

To light memory of Nodar Chiabrishvili, inexorably
faithful to science, knight of honour and conscience.

On the Characteristic Functions and Parameters of Different Kind of Thermodynamic Systems: Experiment, Observation, Theory

Anzor I. Gvelesiani

*Mikheil Nodia Institute of Geophysics of Iv. Javakhishvili Tbilisi State University
1, Alexidze Str., 0160 Tbilisi, Georgia, e-mail: <anzor_gvelesiani@yahoo.com>*

ABSTRACT

The paper consists own results of laboratory experiments, results of wellknown other works using by us for introduce corrections and interpretations of some of them proceed from common point of view. There are discussion and comparison all of them with each other, in the light of classical works. In the first part of the article, briefly, is given the original laboratory bubble boiling method for modeling (BBMM) of vertical convective motion of two phase homo- and heterogeneous fluids (Georgian natural waters were investigated. The rest part of paper is devoted to the studying of thermodynamic parameters of systems, studying in geophysics and other ranges of science, technology, metallurgy, physical chemistry. In particular, except above-mentioned water solution, there are considered phase transformation processing in the following way: crystal \rightarrow liquid \rightarrow vapour and in the opposite direction. Thus, it is obtained similarity between: (1) Van-der-Waals (P,V)-phase diagram, stress-strain diagram (σ/ϵ), modelling earthquakes, and reconstructed by us figures (MPa/porosity) and (C_p^{-1}, T)-reverse heat capacity-temperature diagram for glycerin, $C_3H_8O_3$, and (h, E)-, dependence between depth of cosmic rays penetration into the Earth atmosphere and their energy; (2) space-time change of parameters of cosmic rays, solar wind, $F_{10.7}$ and ultra-violet radiation, and temperature-time change of nucleation of melted piperin, $C_{17}H_{19}NO_3$, in glass-like crystal state, and sulfides, arsenides, sulfates; (3) change of number of sunspots, W, and geomagnetic activity, c_p , in time, reconstructed by us (here), are in a good agreement with ($\Delta T, t$); (4) (BBMM) bubble-boiling method, may be used for modelling of vertical convection, first of all, in the geo- and solar atmosphere; theoretically is confirmed our conclusion about Van-der-Waals-type and Tammann-type thermodynamic phenomena in geophysical spheres, metallurgical and physico-chemical investigations. It is necessary to note that well known Tammann's curve is not Gaussian one.

Keywords: glass-like state, convection, thermodynamic system, phase, bubble boiling, nucleation, magma, volcano, cosmic rays, magnetic field, solar wind, sunspot, alloys, modelling.

1. Introduction

It is necessary to note that every review and last monographs, devoted to the geophysical problems are ended with words about urgent necessity of new experimental investigations all the more that thermodynamics first of all is experimental science. Vertical motion of the thermals in different geophysical spheres: in the atmosphere, oceans, mantle, Earth's liquid core etc., caused by the Archimedes force in the gravity field is a general element of any scale of the fluid convective motion. Experimental modelling of this type convective flows is the most actual one in geophysical spheres, different physical-chemical and technical processes equally [1-47].

Thermodynamic laws are empirical exceptionally, therefore they may be considered with using different ways, which, of course, are equivalent. It would be great mistake to be carried away the mathematics and forget about physics [15]. In this article, it is analyzed results of discussion some published important works and our investigation of thermodynamic parameters of natural waters of Georgia. Even this simplest case of vertical one-dimensional two-phase motion reveal a rich wealth of hydrodynamic regimes and phenomena. It is necessary to note that we did not discover any case of an infringement of the linear law of obtained original universal experimental curves (T, t), ($\Delta S, T$), (t, ρ) and (T, ρ) of natural waters or artificial water solutions at the points of the second kind discontinuity. Thus, side by side well-known method of similarity and dimensional analysis, we have new original method, which effectively used in our work, and may be applied to investigation fluids convection in different geospheres: liquid core of the Earth, mantle plumes, magma of volcanoes, thermal and mineral waters, geysers, clouds and thermals in low atmosphere and upper one, cosmic rays, solar wind etc.

2. Construction of original universal experimental curves.

2.1. Fig. 1-5 show temperature-time dependences for natural waters: (1) spring of t. Tsalka (21.5 min), (2) the Black Sea, t. Anaklia (17 min), (3) sulphuric water of the Lake Lisi (14.5 min), (4) sulphuric waters of the old Tbilisi bath-houses (11 min); (5) honey water solution (7 min). In brackets given beginning of their bubble boiling moment.

This time signed below as “dsc” – the second kind discontinuity of these curves.

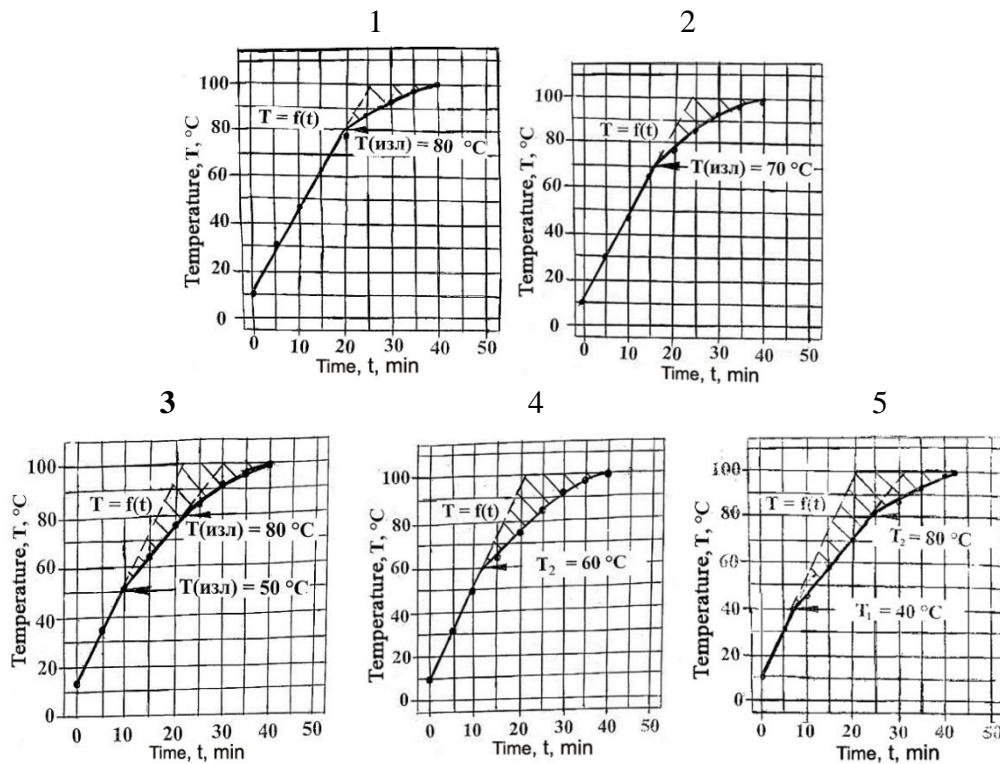
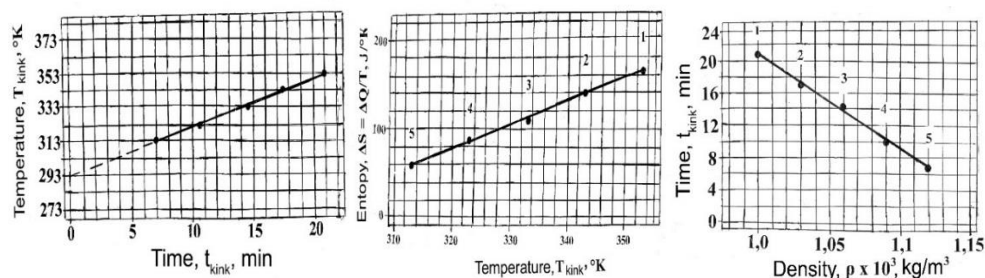


Fig. 1- 5. Experimental dependences (T, t) of heating of natural waters solution and water solution of honey of different density: (1) $\rho = 1.0 \text{ g/cm}^3$, (2) $\rho = 1.02 \text{ g/cm}^3$, (3) $\rho = 1.07 \text{ g/cm}^3$, (4) $\rho = 1.08 \text{ g/cm}^3$; and (5) $\rho = 1.27 \text{ g/cm}^3$.



(a) (b) (c)

Fig. 6. Universal curves of the parameters characterizing the change of bubble boiling regimes: (T, t)_{dsc}, (b) (ΔS, T)_{dsc}, (c) (t, ρ)_{dsc}; **1** - spring of t. Tsalka (21.5 min); **2** - the Black Sea water near t. Anaklia (17 min); **3** - sulphuric water of the Lake Lisi (14.5 min); **4** - sulphuric waters of the old Tbilisi bath-houses (11 min); **5** – water solution of honey (7 min).

Dependences of investigated liquids thermodynamic characteristics in points of the second kind of discontinuity (dsc): (T,t)_{dsc}-, (ΔS, T)_{dsc}-, (t, ρ)_{dsc}- curves have linear character (Fig. 6). For example, empirical formulas at a power of heating the vessel with liquid of optimal volume [22] of (T, t)_{dsc}-, (ΔS, T)_{dsc}-, and (t, ρ)_{dsc}, of (Fig. 6a,b,c) are following:

$$T_{dsc} = T_0 + \alpha \Delta t_{dsc1}, \quad T_0 = 293 \text{ K}, \alpha = 2.86 \text{ K/min}; \quad (1)$$

$$\Delta S_{dsc} = \Delta S_0 + \beta T_{dsc}, \quad \Delta S_0 = 60 \text{ J/K}, \beta = 2.7 \text{ J/K}^2; \quad (2)$$

$$(\rho_{dsc} - 1)/a + t_{dsc}/b = 1, \quad a = 0.18 \text{ g/cm}^3, b = 21.5 \text{ min}. \quad (3)$$

Represented below (ΔS, T)- and (T, t)-curves very clearly show the points of the second kind of discontinuity.

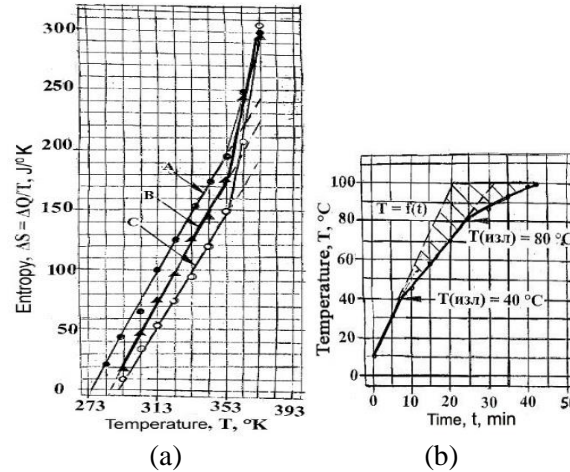


Fig. 7. (a) (ΔS, T) – entropy-temperature dependence: at the heating intensities: q = 75 J/s (A- branch); q = 47 J/s (B-branch), and q = 35 J/s (C-branch), respectively; (b) (T, t) – temperature-time dependence for q = 47 J/s).

As it is seen, Fig. 7 shows that: (a) (ΔS, T)- curves have only one, (T₂)_{dsc}, point of discontinuity while (b) (T, t)-curve has two points of the dsc, T_{1, dsc} = 40 °C = 313 K, and T_{2, dsc} = 80 °C = 353 K. If (ΔS, T)-dependence to express in degrees of °C for T₀ > 10 °C, then in this dependence is revealed the T_{1, dsc} = 40 °C = 313 K, too. A- and B- branches coincide. At T₀ ≤ 10 °C, if in formula ΔS = ΔQ/T the temperature were taken in °C (instead of °K), then the entropy “does not loose” the first point of discontinuity, T_{dsc} = 40 °C. This may be allow us to expand the laboratory method of modeling the convection in different geophysical environments for obtaining of dsc-points. BBMM method allows us to definite a density, at least, of any substance water solution using our universal experimental (T, /ρ)_{dsc} curve.

Thus, test of artificial natural and mineral waters solutions, shows, for example, that measuring of temperature near the break (discontinuity) point (during some minutes after completion) were enough to obtain sufficiently full information about change of bubble boiling regimes, unknown density of solution etc. Thus, the proposed method of bubble boiling allows during 7-20 minutes to determine enough accurately the density of water solution of any substance.

For example, water solutions of laundry salt (NaCl) and honey of the same volumetric density ($\rho = 1.03$ g/cm³) are identical by three measured parameters (T , ρ , t) and calculated entropy $\Delta S(T)$ on the dependence plot $T_{dsc}(\rho_{dsc})$ and $T(t)$. Experiments on specially prepared samples of water solutions of honey with mass multiplicity (0:1:2:3:4:5) g /300 g of water confirmed excellently the discovered pattern (T_{dsc}/ρ_{dsc}): 80°C/1.0 g –70°C /1.0 g –60°C /1.0 g –50°C /1.0 g –40°C /1.0 g (compare with Fig. 5c (!)).

2.2. Let us calculate a quantity of heat (Q) conducting through the side of cylindrical glass

$$dQ = \lambda \frac{T - T_{air}}{d} S_{side},$$

temperature (constant along the height (h) of the glass), T_{air} is the laboratory air temperature practically maintained constant before the end of bubble boiling process (100°C) at the condition of where λ is the heat conductivity of the glass; d is the thickness of the glass side; T is glass temperature at an open window of the laboratory. Thus, we have

$$Q = -\lambda \frac{dT}{dr} 2\pi R_{bot} h, \quad (4)$$

where dT/dr is an air temperature gradient at the side of glass, R_{bot} is a radius of the glass bottom, h is the height of water in the glass. There are possible two cases: (a) $dT/dr < 0$ or (b) $dT/dr = 0$. Then, in the first case

$$Q_1 = mc \Delta T + \Delta m L + \lambda \frac{dT}{dr} 2\pi R_{bot} h + Mc' \Delta T; \quad (5)$$

in the second one we have (it is suggested that there is not a heat flux through the side of the glass)

$$Q_2 = mc \Delta T + \Delta m L + Mc' \Delta T, \quad (6)$$

where $M = 300$ g is the mass of the glass; $c' = 0.779$ J / (g · K) is the glass heat capacity; for usual glass, $\lambda_1 = 0.7$ J / (m · s · K) = 0.007 J / (cm · s · K); and for quartz glass, $\lambda_2 = 1.36$ J / (m · s · K) = 0.0136 J / (cm · s · K); $\Delta T = 90^\circ\text{C}$; $d = 0.3$ cm; $S = \pi R^2$, $h = 8$ cm, $m = 300$ g; $\Delta m = 30$ g; $R_{bot} = 3.45$ cm; $\rho = 1$ g / cm³; $c = 1$ cal / g · K = 4.19 J / (g · K); $L = 2.25 \cdot 10^3$ J / g; $W_0 = 103$ J / s, $W_{bot} = 47$ J / s.

Substituting the numerical values of parameters of ambient and researched thermodynamic object into above-mentioned expressions for thermo-balance gives following results:

$$Q_1 = (300 \cdot 4.19 \cdot 90 + 30 \cdot 2.25 \cdot 10^3 + 0.007 \cdot (90 / 3) \cdot 2\pi \cdot 3.45 \cdot 8 + 185 \cdot 0.779 \cdot 90) \text{ J} = \\ (113130 + 67500 + 36.4 + 12970.35) \text{ J} = 193636.75 \text{ J};$$

$$Q_2 = (113130 + 67500 + 12970.35) \text{ J} = (180630 + 12970.35) \text{ J} = 193600.35.$$

or

$$Q_1 = 193636.75 \text{ J}; \quad Q_2 = 193600.35.$$

As it is seen, a loss of a heat through the sides of the chemical glass is infinitesimal and is equal to 0.02 %.

$$Q'_1 = (300 \cdot 4.19 \cdot 90 + 30 \cdot 2.25 \cdot 10^3 + 0.0136 \cdot (90 / 3) \cdot 2\pi \cdot 3.45 \cdot 8 + 185 \cdot 0.779 \cdot 90) \text{ J} = \\ (113130 + 67500 + 72.8 + 12970.35) \text{ J} = (180630 + 72.8 + 12970.35) \text{ J} = 193673.15 \text{ J};$$

$$Q'_2 = (300 \cdot 4.19 \cdot 90 + 30 \cdot 2.25 \cdot 10^3 + 185 \cdot 0.779 \cdot 90) \text{ J} = (113130 + 67500 + 12970.35) \text{ J} = \\ (180630 + 12970.35) \text{ J} = 193600.35 \text{ J}.$$

or

$$Q'_1 = 193673.15 \text{ J}; \quad Q'_2 = 193600.35 \text{ J}.$$

2.3. Step-by-step calculation of heat balance (T_0 , T'_{dsc} , T''_{dsc} , T_b , t).

2.3.1. (T_0 , T'_{dsc} , t) Thermal mode and the smallest bubbles.

$T_0 = 10^\circ\text{C}$, $T'_{dsc} = 40^\circ\text{C}$, $t = 7$ min.

$$Q_{11} = (300 \cdot 4.19 \cdot 30 + 0.007 \cdot (30 / 3) \cdot 2\pi \cdot 3.45 \cdot 8 + 185 \cdot 0.779 \cdot 30) \text{ J} = (37710 + 12.1 + 432.3) \text{ J} = 38154.4 \text{ J};$$

$$Q_{21} = (37710 + 432.3) \text{ J} = 38142.3 \text{ J}.$$

$$Q_{11} = 38154.4 \text{ J}; \quad Q_{21} = 38142.3 \text{ J}.$$

2.3.2. ($T'_{\text{dsc}}, T''_{\text{dsc}}, t$) Transform to mode of large bubbles.

$T'_{\text{dsc}} = 40^{\circ}\text{C}$, $T''_{\text{dsc}} = 80^{\circ}\text{C}$, $t = (25 - 7) \text{ min} = 18 \text{ min}$.

$$Q_{12} = (300 \cdot 4.19 \cdot 40 + 0.007 \cdot (40 / 3) \cdot 2\pi \cdot 3.45 \cdot 8 + 185 \cdot 0.779 \cdot 40) \text{ J} = (50280 + 16.12 + 576.4) \text{ J} = 50872.52 \text{ J};$$

$$Q_{22} = (50280 + 576.4) \text{ J} = 50656.4 \text{ J}.$$

$$Q_{12} = 50872.52 \text{ J}; \quad Q_{22} = 50656.4 \text{ J}.$$

2.3.3. (T''_{dsc}, T_b, t) regime of the largest bubbles.

$T''_{\text{dsc}} = 80^{\circ}\text{C}$, $T_b = 100^{\circ}\text{C}$, $t = (42.5 - 25) \text{ min} = 17.5 \text{ min}$.

$$Q_{13} = (300 \cdot 4.19 \cdot 20 + 30 \cdot 2.25 \cdot 10^3 + 0.007 \cdot (20 / 3) \cdot 2\pi \cdot 3.45 \cdot 8 + 185 \cdot 0.779 \cdot 20) \text{ J} = (25140 + 67500 + 8.06 + 288.2) \text{ J} = 92936.26 \text{ J};$$

$$Q_{23} = (25140 + 67500 + 288.2) \text{ J} = 92928.2 \text{ J}.$$

$$Q_{13} = 92936.26 \text{ J}; \quad Q_{23} = 92928.2 \text{ J}.$$

2.4. Now consider the dependence of liquid overheat by its heating from below at the bottom of the flask on the intensity of liquid boiling away ($\Delta m/\Delta t$). What is the temperature (T) of the flask bottom?

Heat amount, $q = \Delta Q/\Delta t$, coming in a unit of time from a heater through the flask bottom in the water, equals to:

$$\Delta Q/\Delta t = \lambda(T - T_b)S/d, \quad (7)$$

where T_b – the boiling point of water, λ – the coefficient of thermal conductivity of glass, d – thickness of glass at the bottom of vessel, S – the area of the flask bottom.

Suppose, all input energy in the flask is discharged on water evaporation

$$L\Delta m = W \Delta t, \quad (8)$$

here L – hidden heat of vapor formation, Δm – evaporated during the time Δt the mass of water, W – heater power (J/s).

From here we have

$$T = T_b + \frac{dL\Delta m}{\lambda S\Delta t}, \quad (9)$$

or

$$T = T_b + d \cdot W / (\lambda \cdot S), \quad (10)$$

Overheat of bottom layer of water in the flask can be expressed as:

$$\Delta T = d \cdot W / (\lambda \cdot S), \quad (11)$$

where $\lambda \approx 0.7 \text{ W}/(\text{m} \cdot \text{K}) = 1/600 \text{ cal}/(\text{cm} \cdot \text{K})$; $d = 0.3 \text{ cm}$, $S = \pi R^2$, $h = 8 \text{ cm}$, $m = \pi R^2 h \rho = 300 \text{ g}$; $\rho = 1 \text{ g}/\text{cm}^3$, $c = 1 \text{ cal}/\text{g} \cdot \text{K}$, $= 103 \text{ J}/\text{s}$.

Using above mentioned characteristics of our thermodynamic system we obtain

$$\Delta T = d \cdot P / (\lambda \cdot S) = 0.3 \cdot 103 / (0.7 \cdot 300/(8 \cdot 1)) \approx 1.18^{\circ}\text{C}. \quad (12)$$

First bubbles of large size (beginning of fluid bubble boiling process) (the temperature of water in a volume at first 5 min was 30 °C) appears during overheat of bottom layer of water in the flask, heated from below on the electric hot plate, $\Delta T \approx 1.18$ °C. Then, after 5 min measured temperature was equal to 40 °C and so on.

2.5. Initial fluid temperature in the flask was always equal to the air temperature in the laboratory of thermal vacuum chamber $T = 10$ °C (winter period). Based on the investigated by us original method of bubble fluid boiling the series of experiments has been performed to investigate thermodynamic parameters of natural waters in Georgia (thermal waters, mineral waters, mountain springs, sea and lake waters) and artificial solutions. To complete the thermodynamic picture we calculate, in the system of units S, total amount of heat, transferred to liquid thermodynamic system in time $\Delta t = 2400$ sec, starting at initial temperature of $T_0 = 10$ °C to the moment $T_k = 100$ °C, intense bubble boiling, $\Delta Q = mc (T_k - T_0) = 0.3 \cdot 4.2 \cdot 10^3 (100 \text{ °C} - 10 \text{ °C}) = 113.4$ kJ. After dividing the received heat on time $\Delta t = 2400$ sec, we get for intensity of heat $q = \Delta Q / \Delta t$ of an investigated object the value $q = 47$ J/sec. Compatible our calculations with observations in Iceland [16].

2. 6. Geysers. Geophysical peculiarities.

Geysers are underground reservoirs filled with ground water and heated by intense source of heat below the surface. The exit of them to the surface is going through a narrow channel, in the "quiet" period almost completely filled with water. "Active" period comes when water boils in the underground reservoir, and during the eruption of the geyser a channel is almost completely filled only with vapor, which is released outside. We'll estimate what a part of water is lost during one release. (The height of vapor fountain is $h_2 = 10$ m), if at the depth of geyser channel $h_1 = 37$ m water is heated up to 140°C.

Let's consider that specific temperature q of water vapor $L = 2.25 \cdot 10^6$ J/kg. Atmospheric pressure is normal, $P_0 = 1.015 \cdot 10^5$ Pa.

Liquid starts boiling at the moment when the pressure of saturated vapor inside the bubbles of gas (which are in liquid) becomes equal to external pressure. In our case pressure differs from the atmospheric one by the value of hydrostatic pressure created by water column in the geyser channel. Therefore, the water temperature in the geyser reservoir must be higher by the value of ΔT than the temperature of boiling water under the normal pressure, equal to 100°C.

When water column in a channel at the time of water boiling is released outside, vapor pressure and liquid temperature are decreased up to atmospheric pressure and the boiling point at normal pressure, i.e. up to 100°C. Amount of heat $mc\Delta T$ released during temperature drop of all water mass in a reservoir is used for evaporation of some part Δm and message about its potential energy equal to $\Delta mg (h_1 + h_2)$.

We note that "active" period of geyser is very rapid and takes relatively short time (compare with the intensive bubble boiling process in the laboratory vessel with water or any liquid). "Quiet" period is more long process where repeated warm-up of all water mass in the underground reservoirs happens through thermal conductivity. Water mass by the underground water inflow restores its initial reserve.

The heat sink at the moment of eruption can be neglected and we can consider that eruption happens by the internal energy of water in geyser reservoir.

We have

$$mc \Delta T = \Delta m [L + g (h_1 + h_2)], \quad (13)$$

where L is a latent heat of the water evaporation.

For $\Delta T = 140^\circ\text{C} - 100^\circ\text{C} = 40^\circ\text{C}$, $c = 4.19$ kJ/(kg · K), $L = 2.25 \cdot 10^6$ J/kg

$$\frac{\Delta m}{m} = \frac{c\Delta T}{L + g(h_1 + h_2)} \approx \frac{c\Delta T}{L}, \quad \frac{\Delta m}{m} 100\% \approx 7.5 \%. \quad (14)$$

3. Ocean. Heat flux. Geophysical peculiarities [20].

3.1. The surface layers of the acting ocean are stirred by the winds and undergo a regular cycle of convection and restratification in response to the annual cycle of buoyancy fluxes at the sea surface. The buoyancy flux, B , is expressed in terms of heat and fresh water fluxes as

$$B = \frac{g}{\rho_0} \left(\frac{\alpha_\theta}{c_w} H + \rho_0 \beta_s S (E - P) \right), \quad (15)$$

where $c_w = 3900 \text{ J Kg}^{-1} \text{ K}^{-1}$ is the heat capacity of water, H is the surface heat loss, $E - P$ represents the net fresh water flux (evaporation minus precipitation). Over the interior of the ocean basin, heat fluxes rise to perhaps 100 W m^{-2} in winter, and $E - P = 1 \text{ m yr}^{-1}$, implying a buoyancy flux $B \sim 10^{-8} \text{ m}^2 \text{ s}^{-3}$. Unlike the upper regions of the main thermocline where mixed layer $h \leq 10^2 \text{ m}$, at the **convection** sites the stratification is sufficiently weak, $N/f \approx 5-10$, and the buoyancy forcing is sufficiently strong, $\geq 10^{-7} \text{ m}^2 \text{ s}^{-3}$, corresponding to heat fluxes as high as 1000 W m^{-2} , convection may reach much greater depths $h > 2 \text{ km}$. This results were discussed in our article [24].

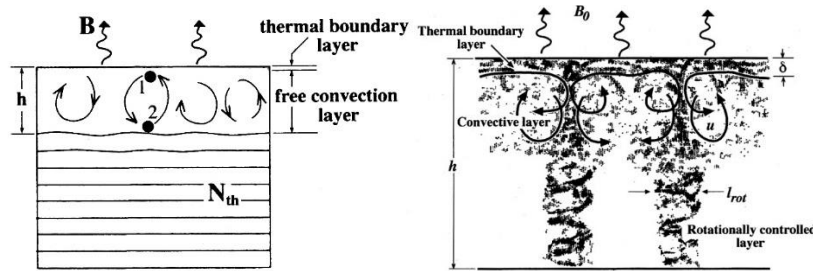


Fig. 8a. Convection in an ocean surface turbulent layer according to [20].

3.2. Convective phenomena of conductive fluid placed in external magnetic field (see ref. of [44]) and in the convective zone of the solar atmosphere under the photosphere [37]. Compare turbulent layers on surface of ocean (Fig. 8a) and zone of convection in the solar atmosphere (Fig. 8b).

Below are adduced some other results, where effect of the magnetic buoyancy is seen clearly both: (a) calculation of the plane solar magnetic field (sunspots), [44], and (b) the space solar wind, [49].

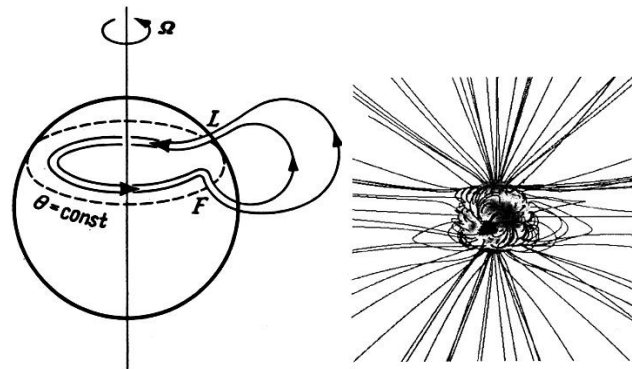


Fig. 8b. Pictures: (1) – formation of sunspots by the solar toroidal magnetic field, according to Parker (1955), [50]; (2) three-dimensional solar wind, according to Neugebauer (1999), [49].

4. Van der Waals-like a brittle fracture (σ/ϵ) -dependence, according to [19, 27].

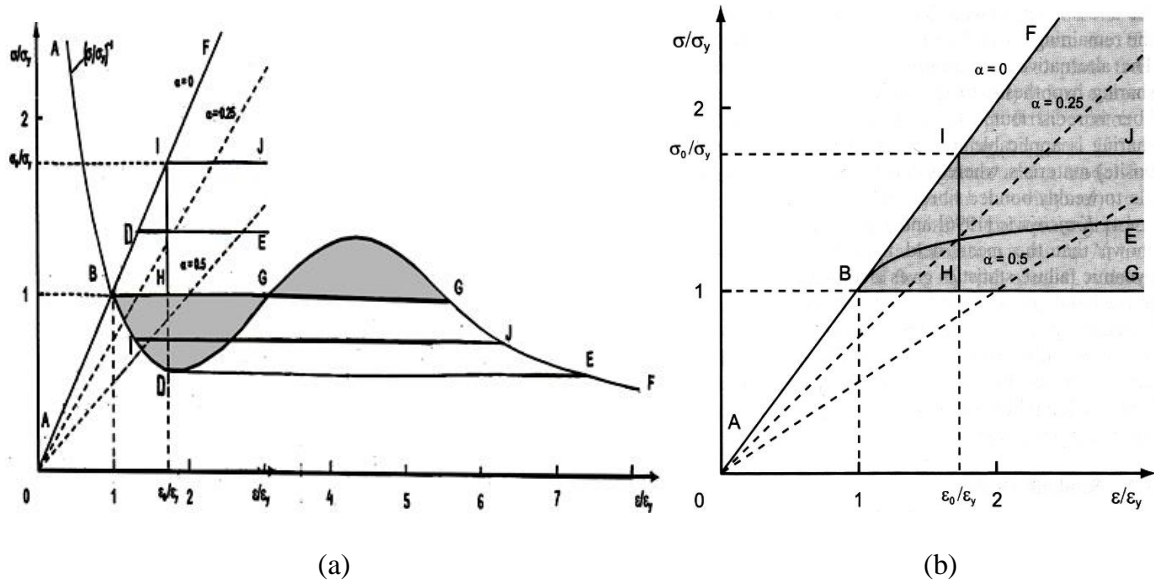


Fig. 9. (a): Van der Waals' pressure-volume (P, V)- type diagram the $((\sigma/\sigma_y)^{-1}, (\epsilon/\epsilon_y))$ -one [27]; and (b): stress-strain $((\sigma/\sigma_y), (\epsilon/\epsilon_y))$ -diagram for a brittle solid [19].

The author of [19] sees the similarity between the diagram of the stress-strain process which take place in the rocks during the earthquakes and the pressure-volume one of water-vapor phase transformation during the bubble boiling process [27] (compare with above mentioned our BBM method [21-25] and Figs. 10-12).

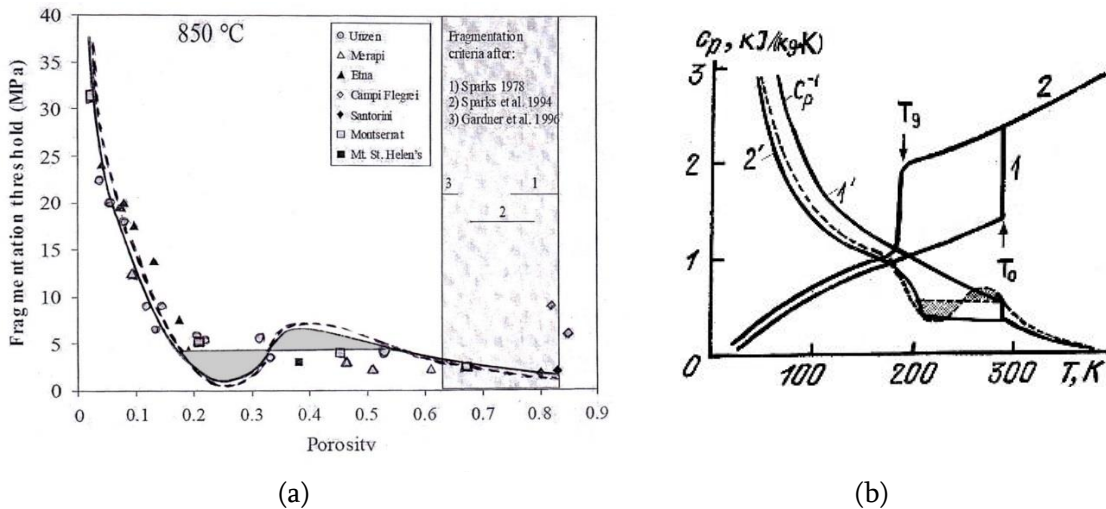


Fig. 10. (a) – Results of [17], after remake, show Van der Waals-type “metastable” parts of the curve when right-side experimental points were taken into account. (b) – (C_p, T) - and (C_p^{-1}, T) -reverses heat capacity-temperature diagram for glycerin, $C_3H_8O_3$, (see ref. of [46]).

As can be seen, the experimental plots of the dependences of mirror reflection of some of parameters: (S, t) , (S, V) , (q, p) (N, t) , (σ, ϵ) , (τ, p) in the processes of phase transformation (boiling, glassy state etc.) demonstrate the “Van der Waals”- and “Andrews”-type forms (see [17, 19] and Figs. 9 -12a).

4.2. The samples used in the present study were collected at seven different volcanoes or volcanic centers and represent a broad range of composition and porosity (2 - 85 vol.%). The experimental data (representing approx. 400 experiments) show a strong relation between porosity and the fragmentation threshold at 850 °C. (Note that porosity/100 is plotted at the x-axis.) The grey box shows the range of different earlier fragmentation criteria defined by bubble coalescence [34] and shear induced foam instability [35].

5. Tammann curve's-type of nucleation of piperin crystals in glassy state [36].

This form of experimental curves proved to be very important in the present side by side Van der Waals one. Both of them plays important role in different scientific and technical spheres.

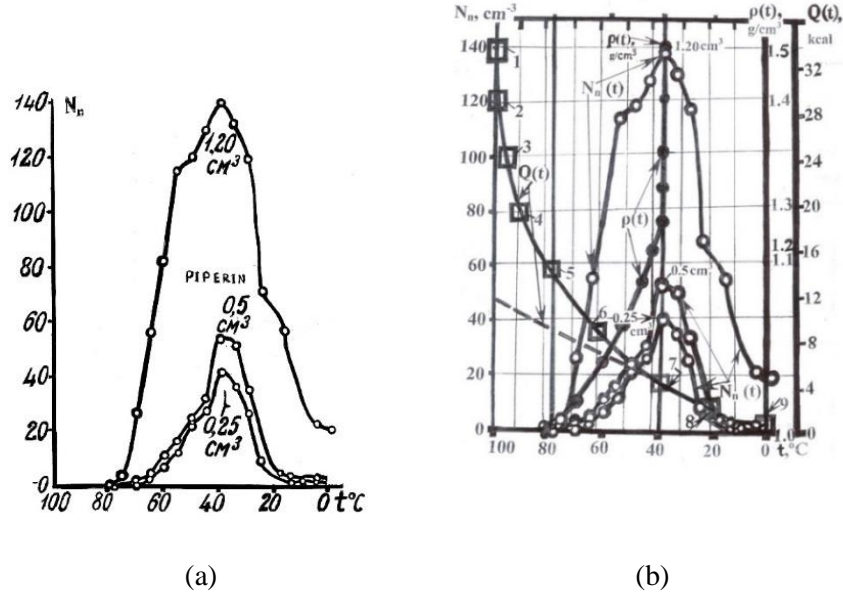


Fig.11. (a) Tammann's (N_n, t)-piperin nucleus number-temperature curves [36];
 (b) shows the Tammann's (N_n, t)-curve in center and added $\rho(t)$ - and $Q(t)$ -curves for different natural waters and artificial solutions of different concentration.

It is very interesting to note that Tammann's exactly this, (40–80) °C, temperature interval of piperin crystals nucleation ([36]) coincides with the curves $(T, t)_{dsc}$ of Fig. 1-5 having the "dsc" points of discontinuities in the same (40–80) °C interval, [21-25]. Fig. 11 shows the temperature change of glycerin in crystal (1) and in glassing liquid (2) states at the normal atmosphere pressure, respectively. T_0 is the equilibrium temperature of melting and T_g is the temperature of the glassy structure formation.

For the rate of the crystal nucleation, J , in the supercooled melts we use simplified formula [6]:

$$Jdt = K \exp\left(-\frac{u_i}{kT}\right) \exp\left(\frac{A_s}{kT}\right) dt, \quad (16)$$

where u_i is the energy of activation of phase transformation $I \rightarrow II$, A_s – minimal free surface energy of the crystal form, K is constant, T is temperature, k is Boltzman's constant. For nucleus of spherical shape and averaged Q_s , σ , and d , instead of (16) we have

$$Jdt = K \exp\left\{-\left[\frac{u_i}{kT} + \frac{B}{(T_s - T)^2 T}\right]\right\} dt, \quad \left(B = \frac{4\omega}{3k} \left(\frac{M}{d}\right)^2 \frac{\sigma^3 T_s^2}{Q_s^2}\right). \quad (17)$$

Now, though the values of u_i and B are unknown in every separate case, nevertheless, one may define the bounds of their values, if instead of unknown the boundary energy crystal/melt in the expression of B , (17), were taken the surface tension. Calculations showed that theoretical (J, T) -curve [6] has the same shape as obtained by Tammann and his pupils on the base of numerous experiments [36].

Below Van der Waals' and Tammann's-type curves (Fig. 12) and (Fig. 13) are represented, respectively. They are in accordance with suggested classification of geophysical phenomena by force of their thermodynamic nature. In Fig. 12 upper curves of ion intensity-years (I, Y) arrange [as (P, V) for temperature, growing from below upwards before critical point in case of real gases (in thermodynamics)] and for h, depth of ions penetration into the Earth atmosphere (in case of cosmic rays). Visually behaviors of above described ion phenomena are similar. The lower, sunspot-years (W, Y) - and geomagnetic activity-years (C_p, Y)-curves are in a good accordance with each other during solar 11-year cycle (1950-1951). It would be interesting to attract once more Fig. 8b, Fig. 11 and Fig. 12.

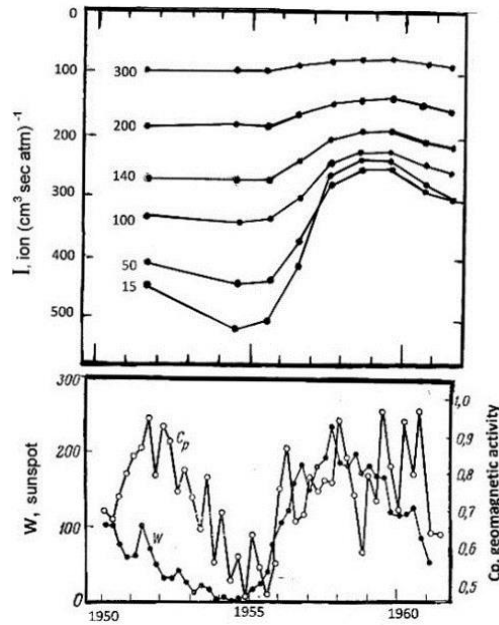


Fig. 12. Values of W, I, C_p – sunspots, cosmic rays intensity at different depths of penetration into atmosphere, geomagnetic activity during 1950 -1961 (Neher, Anderson, 1962; Thule, Greenland, AB USA).

To the Tammann'-type curves are belonged the curves the Solar F_{10.7} and UV- ultra-violet radiation as it is clearly seen from Fig. 13. And not only the very hot solar plasma radiation, but also, of all hot alloys structural and thermal parameters have the same, Tammann character (Fig. 14-17).

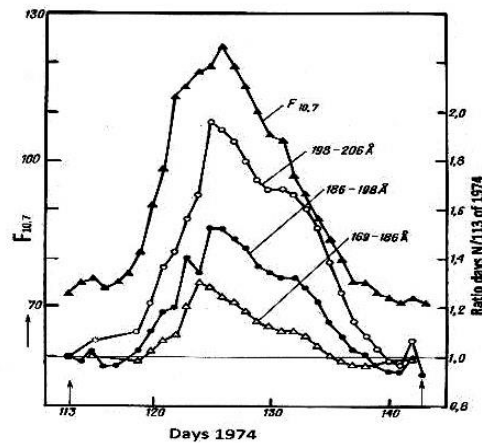


Fig. 13. Correlation of extreme ultraviolet with F_{10.7} (Manson, 1976)

At last, consider some results from monograph [43], devoted to transformation of sulphides, arsenides and sulphates under mechanical and thermal influences. Obtained there graphical illustrations about structural and thermal characteristics of natural or artificial samples are also just Tammann's-type curves. Compare calculated, according to the formula (17), crystal nucleation-temperature (J, T)-dependence [6], Fig. 14-16, Fig. 11, 13 and Fig. 17.

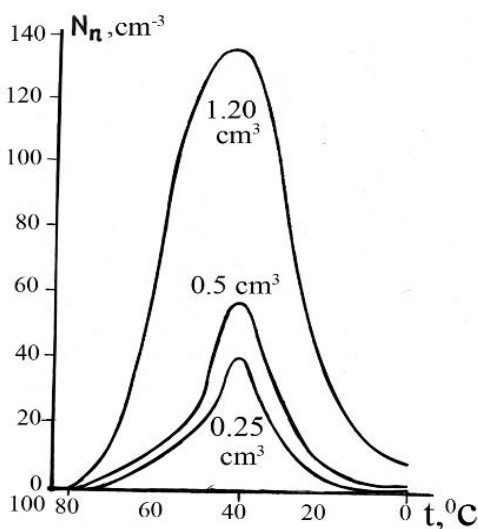


Fig. 14. Theoretical curve of intensity of crystal nucleus against temperature of supercooled melt according to [6] was used by us in order to construct Tammann's well-known experimental curve for piperin (Fig. 11) [36].

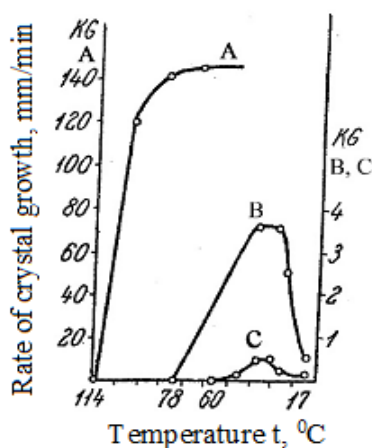


Fig. 15. Temperature dependence of crystallization rate of acetanilide –dinitrophenol benzyl [36]. A–acetanilide; B–binary eutectic of acetanilide with dinitrophenol; C–ternary eutectic. All of them are Tammann's-type curves, as we see, too.

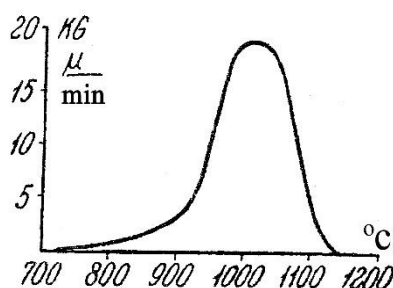


Fig. 16. The rate of spherulit glass needles growth against the temperature ((RG,T) -dependence.

The length of spherulit needles measured by means of microscope and rate RG_{\max} was $\sim 20 \mu/\text{min}$ (ref.[36]).

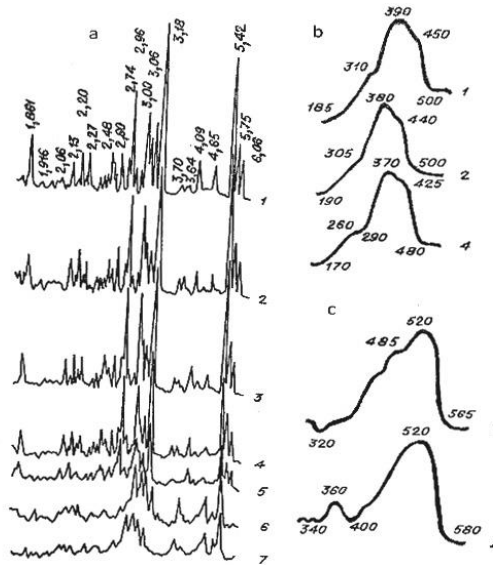


Fig. 17. Structural and thermal characteristics of realgar (As, S) and products of its mechanical processing. 1 – initial, 2-7 – activated (min) in 2-5 – water (0.5; 2; 7; 15), 6 –air (7), 7 – combined (14) environments; a diffractograms; b, c – DTA-curves (platinum and quartz crucible furnaces) [36].

6. Conclusions.

Thus, it is obtained similarity between: (1) Van-der-Waals (P/V)-phase diagram [19], stress-strain diagram (σ/ϵ), modelling earthquakes [27], and reconstructed by us figures (MPa/porosity) [30-34] and (C_p^{-1}, T)-reverse heat capacity-temperature diagram for glycerin, $C_3H_8O_3$, [46] and (h, E)-, dependence between depth of cosmic rays penetration into the Earth atmosphere and their energy [42,41]; (2) space-time change of parameters of cosmic rays, solar wind, $F_{10.7}$ and ultra-violet radiation, [37-42] and temperature-time change of nucleation of melted piperin, $C_{17}H_{19}NO_3$, in glass-like crystal state, [36], and sulfides, arsenides, sulfates, [43]; (3) change of number of sunspots, W, and geomagnetic activity, c_p , in time, [42], reconstructed by us (here), are in a good agreement with (ΔT , t), [25]; (4) (BBMM) bubble-boiling method [21, 22] may be used for modelling of vertical convection, first of all, in the geo- and solar atmosphere, [21-25]; theoretically is confirmed our conclusion about Van-der-Waals-type and Tammann-type thermodynamic phenomena in geophysical spheres, metallurgical and physico-chemical investigations. It is necessary to note that well known Tammann's curve is not Gaussian one.

References

- [1] Wallis G. B. One-dimensional two-phase flow. McGraw Hill Book Company, New York-San Louis-San Francisco-London- Sydney-Toronto-Mexico-Panama, 1970.
- [2] Thomson J. On a changing tessellated structure in certain liquids. Proc. Philos. Soc. Glasgow, v. 13, 1882, pp. 464-468.
- [3] Bénard M. Les tourbillons cellulaires dans une nappe liquide. Revue generale des Sciences pures et appliquee, v. 11, 1900, pp. 1261-71 and 1309-28.
- [4] Chandrasekhar S. Hydrodynamic and hydromagnetic stability. Clarendon Press, Oxford, England, 1961, 652 p.
- [5] Gibbs J. W. Thermodynamics. Statistical Mechanics. Moscow, Nauka, 1982, 584 p. (in Russian).

- [6] Volmer M. Kinetik der Phasenbildung. Dresden-Leipzig: Steinkopf, 1939, 220 p.
- [7] Frenkel Ya. I. Kinetic theory of liquids. Leningrad, Leningrad Department, Nauka, 1975, 592 p. (in Russian).
- [8] Zel'dovich Ya. B. On the theory of new phase formation. JETP, 1942, T. 12, vip. 11-12, pp. 525-538, (in Russian).
- [9] Kagan Yu. O kinetike kipenia chistoy zhidkosti. Zhurnal fizicheskoy khimii. T. XXXI, № 1, 1960, pp. 92-101, (in Russian).
- [10] Skripov V. P. Metastable Liquids. M.: Nauka, GRFML, 1972, 312 p. (in Russian).
- [11] Ermakov G. V., Lipnjagov E. V., Perminov C. A. New criterium for comparison of classic. T. 16, № 4, 2009, pp. 695-699, (in Russian).
- [12] Golitsyn G. S. Energy of convection. Non-linear waves: Stochasticity and Turbulence. Gorky: AN SSSR, IPF, 1980, pp. 131-139, (in Russian).
- [13] Boubnov B. M., Golitsyn G. S. Convection in rotating fluids. J. Fluid Mech., 1995, v. 219, pp. 215-239.
- [14] Brennen Chr. E. Cavitation and bubble dynamics. University Press, 1995, 64 p.
- [15] Kubo R. Thermodynamics. An advanced course with problems and solutions. North Holland Publishing Company–Amsterdam, 1968 (Russian ed.: M.: Mir, 1970, 304 pp.).
- [16] Roberts M. J., Jökulhlaups: A reassessment of floodwater flow through glaciers. Reviews of Geophysics, 2005, 43, RG1002/ 2005, pp. 1-21.
- [17] Zhang Y., Xu Z., Zhu M., Wang H. Silicate melt properties and volcanic eruptions. Reviews of Geophysics, 2007, 45, RG4004/ 2007, pp. 1-27.
- [18] Jellinek A. M., Manga M. Links between long-lived hot spots, mantle plumes, D", and plate tectonics, Reviews of Geophysics., 42, RG3002, 2004, doi: 10.1029/2003RG00014
- [19] Rundle J. B., Turcotte D. L., Shcherbakov R., Klein W., Summis Ch. Statistical physics approach to understanding the multiscale dynamics of earthquake fault system. Reviews of Geophysics, v. 41, N 4, RG4001, 2003, pp. 5.1-5.30.
- [20] Marshall J., Schott F. Open-ocean convection: observations, theory, and models. Reviews of Geophysics, 37, 1 / February, 98RG02739, 1999, pp. 1-64.
- [21] Gvelesiani A. I. To the problem of one-dimensional two-phase/many-component flow in different geophysical mediums. J. Georgian Geophys. Soc., v.16B, 2013, pp. 118-127.
- [22] Gvelesiani A., Chiabrishvili N. Laboratory modeling of thermals generation in geophysical environment by means of bubble boiling method. J. Georgian Geophys.Soc., v.16B, 2013, pp. 128-136.
- [23] Gvelesiani A., Chiabrishvili N. Additional experiments about investigation of the peculiarities of the bubble boiling of clear water, H₂O, and sugar, C₁₂H₂₂O₁₁, and edible salt, NaCl, water solutions of different densities. J. Georgian Geophys. Soc., v.17A, 2014, 132-139.
- [24] Gvelesiani A. Open thermodynamic systems: convection and similar processes modeling by the only fluids bubble boiling method. J. Georgian Geophys. Soc., v.17B, 2014, pp. 38-57.
- [25] Gvelesiani A., Chiabrishvili N. Study of Georgian natural waters thermodynamic parameters behavior by means of original fluids bubble boiling method. J. Georgian Geophys. Soc., v.18B, 2015, pp. 52-63.
- [26] Silvestri M. Hydrodynamics and heat exchange at drop-annular regime of two-phase flow. In book: Advances in Heat Transfer. (Ed. by T. F. Irvine, J. P. Hartnett), AP, New York-London, v. I, 1964.
- [27] Debenedetti P. G. Metastable Liquids. Princeton Univ. Press, Princeton, N. J., 1996.
- [28] Skripov V. P., Koverda V. P. Spontaneous crystallization of super-cooled liquids. M.: Nauka, GRFML, 1984, 232 p. (in Russian)
- [29] Dergarabedian P. The rate growth of vapor bubbles in superheated water. J. Appl. Mech., 1953, pp.537-545.
- [30] Spieler O., Kennedy B., Kueppers U., Dingwell D. B., Scheu B., Tuddeucci J. The fragmentation threshold of pyroclastic rocks. Earth Planet. Sci. Lett., v. 226, 2004, pp. 139-148.
- [31] Sparks R.S.J., The dynamics of bubble formation and growth in magmas: a review and analysis, J. Volcanol. Geotherm. Res., 28, 1978, pp. 257-274.
- [32] Sparks R.S.J., J. Barclay, C. Jaupart, H.M. Mader, J.C. Phillips, Physical aspects of magma degassing. I. Experimental and theoretical constraints on vesiculation, Rev. Mineral. 30, 1994, pp. 414-445.
- [33] Gardner J.E., R.M.E. Thomas, C. Jaupart, S. Tait, Fragmentation of magma during plinian volcanic eruptions, Bull. Volcanol. v. 58, 1996, pp. 144-162.
- [34] McBirney A.R., T. Murase, Factors governing the formation of pyroclastic rocks, Bull. Volcanol., v. 34, 1970, pp. 372-384.

- [35] Zhang Y., A criterion for the fragmentation of bubbly magma based on brittle failure theory, Nature, v. 402, 1999, pp. 648 – 650.
- [36] Tammann G. Kristallisieren u. Schmelzen, Leipzig, 1903; Die Aggregatzustände, Leipzig, 1922.
- [37] Akasofu S.-I., S. Chapman. Solar Terrestrial Physics. Part I. Oxford, Clarendon Press, 1972.
- [38] Eddington A. S. The internal constitution of the stars. Cambridge Univ. Press, London, 1926.
- [39] Hinterreger H. E. J. Atmosp. Terr. Phys., v. 38, 1976, p. 791.
- [40] Manson J. E. Solar specter between 10 and 300 Å. In book: The Solar Output and its variation. Colorado Associated University Press, Boulder, 1976 (pp. 287-312 Russian ed., 1980).
- [41] Dorman L. I. Cosmic Rays Variations and Study of Cosmos. North-Holland, Amsterdam, 1974.
- [42] Neher H., Anderson V. Cosmic rays of balloon altitudes and the solar cycle. J. Geophys. Res., v. 67, N 4, 1962, pp. 1301-1315.
- [43] Kulebakin V. G. Apply mechanic-chemistry in hydro-metallurgic processes. Novosibirsk: Nauka, SO AN SSSR, Inst. Gorn. Dela, 1988, 272 c.
- [44] Moffatt H. K. Magnetic field generation in electrically conducting fluids. Cambridge: Cambridge University Press. London-New York-Melbourne, 1978, pp. 344 (Russian ed.).
- [45] Spieler O., Kennedy B., Kueppers U., Dingwell D.B. et all. The fragmentation threshold of pyroclastic rocks. Earth and Planetary Sciences Letters, Sep. 30, 226 (1-2), 2004, pp. 139-148.
- [46] Skripov V. P., Koverda V. P. Spontaneous crystallization of super-cooled liquids. M.: Nauka, Gl. red. fiz.-mat. lit., 1984, 232 p.
- [47] Leppert G., Boiling P.K. Advances in Heat Transfer. Academic Press, New York –London, 1964, pp. 142-198.
- [48] Gvelesiani A. On the hierarchy of mesoscale vortexes in the turbulent media. Reports of Enlarged Session of the Seminar of I. Vekua Institute of Applied Mathematics, v. 27, 2013.
- [49] Neugebauer M. The three-dimensional solar wind at solar wind minimum. Reviews of Geophysics, v. 37, N 1/February, RG4001, 1999, pp. 107-127.
- [50] Parker E. N. The formation of sunspots from the solar toroidal field. Astrophys. J., v. 122, 1955, pp. 293-314.

სხვადასხვა ბუნების თერმოდინამიკური სისტემების პარამეტრების და მახასიათებელი ფუნქციების შესახებ: ექსპერიმენტი, დაკვირვება, თეორია

ა. გველესიანი

რეზიუმე

ნაშრომი შეიცავს ლაბორატორიული ექსპერიმენტების ახალ შედეგებს და მათ ინტერპრეტაციას. განზოგადებულია სხვა ავტორების კარგად ცნობილი შედეგები, რომელთა განხილვისას შეგვაქვს სათანადო კორექტივები ერთიანი თერმოდინამიკური კუთხით მოვლენების ფიზიკური შინაარსიდან გამომდინარე, დაყრდნობით კლასიკად ქცეულ შრომებზე, სტატისტიკის შესავალში მოკლედ აღიწერება ჩვენს მიერ შემოთავაზებული ვერტიკალური კონვექციის მოდელირების ბუშტოვანი დულილის მეთოდი (BBMM). ნაშრომის ძირითადი ნაწილი ეძღვნება გეოფიზიკის, ფიზიკა-ქიმიის, მეტალურგიის, ტექნიკის სათანადო დარგების ობიექტების თერმოდინამიკური მახასიათებლების კვლევას. ყურადღების ცენტრშია ფაზური გარდაქმნები: კრისტალი \rightarrow სითხე \rightarrow ორთქლი და პირიქით. და ბოლოს დადგენილია: (1) ვან-დერ-ვაალსის (P,V)-დიაგრამის მსგავსება დამაბულობა-დეფორმაცია (σ, ϵ)-დიაგრამას და დაზუსტებულ ჩვენს მიერ წნევა-ფოროვნება ($\Delta P, (\Delta V/V)$)-დიაგრამა, შებრუნებული სითბოტევადობა-ტემპერატურა (C_p^{-1}, T)-დიაგრამა გლიცერინისათვის, $C_3H_8O_3$, და E ენერჯის მქონე კოსმოსური სხივების დედამიწის ატმოსფეროში h სიღრმეზე შეღწევის (h, E)-დიაგრამასთან; (2) მსგავსება კოსმოსური სხივების, მზის ქარის, მზის $F_{10.7}$ და ულტრა-იისფერი გამოსხივების, პიპერინის, $C_{17}H_{19}NO_3$,

გალღობილი მასის ნუკლეაციის სვლა მინისებრივ მდგომარეობაში და სულფიდების, არსენიდების და სულფატების სტრუქტურულ-თერმიული მახასიათებლების; (3) მზის ლაქების რიცხვის, W , და გეომაგნიტური აქტივობის პარამეტრის, C_p , მზის 11-წლიან ციკლში ცვლილების მრუდები ხარისხობრივად ეთანხმება ჩვენს მიერ მიღებულ ტემპერატურის ცვლილებას დროში, $(\Delta T, t)$, (4) ВВММ-მეთოდი შეიძლება გამოყენებულ იქნას კონვექციური პროცესების განხილვისას გეოსფეროებში, მზის ატმოსფეროში და სხვ. თეორიულად მტკიცდება ჩვენი დასკვნა ვან დერ ვაალსის და ტამანის მოვლენების მსგავსება სხვადასხვა გეოსფეროში, მეტალურგიულ და ფიზიკურ-ქიმიურ პროცესებში. უნდა აღინიშნოს ის გარემოება, რომ ტამანის მრუდს არაფერი აქვს საერთო გაუსის მრუდთან.

О характеристических функциях и параметрах термодинамических систем различной природы: эксперимент, наблюдения, теория

А. И. Гвелесиани

Резюме

Работа содержит собственные новые результаты лабораторных экспериментов и их интерпретаций. Обобщаются хорошо известные результаты других работ, используемых нами для внесения в них корректив термодинамически с единой точки зрения, в свете классических работ. В первой части статьи кратко описываются возможности моделирования вертикальной конвекции в двухфазной многокомпонентной текучей среде лабораторным методом (ВВММ). Остальная часть статьи посвящена исследованию термодинамических свойств объектов геофизических, физико-химических, технических наук, металлургии и др. Установлено: (1) сходство (P/V)-диаграммы Ван-дер-Ваальса с (σ/ϵ) -диаграммой напряжение-деформация и уточнёнными нами диаграммами $(\Delta P/(\Delta V/V))$ давление-пористость и (C_p^{-1}, T) обратная теплоёмкость-температура для глицерина, $C_3H_8O_3$, (h, E) -зависимости глубины проникновения в атмосферу Земли космических лучей от энергии; (2) сходство пространственно-временного хода параметров космических лучей, солнечного ветра, $F_{10.7}$ и УФ радиации Солнца с нуклеацией расплавленной массы пиперина, $C_{17}H_{19}NO_3$, в стеклообразном состоянии, и со структурно-термическими характеристиками сульфидов, арсенидов, сульфатов; (3) графическая зависимость числа солнечных пятен, W , и геомагнитной активности, C_p , от времени, реконструированная нами (здесь), хорошо согласуется с зависимостью $(\Delta T, t)$; (4) оригинальный метод пузырькового кипения (ВВММ), может оказаться полезным для лабораторного и численного моделирования вертикальной конвекции в геосферах и атмосфере Солнца. Теоретически подтверждается наше заключение о сходстве явлений Ван дер Ваальса и Таммана с соответствующими явлениями в различных геосферах, металлургии и физико-химических исследованиях. Необходимо отметить, что хорошо известная кривая Тамманна не есть Гауссова кривая.